J.-L. Martin · A. Migus
G. A. Mourou · A. H. Zewail (Eds.)

Ultrafast Phenomena VIII

Proceedings
of the 8th International Conference,
Antibes Juan-Les-Pins, France, June 8–12, 1992

With 523 Figures

Springer-Verlag
Berlin Heidelberg New York
London Paris Tokyo
Hong Kong Barcelona
Budapest

Contents

Part I Overview and General Prospects

Additive Pulse Modelocking and Kerr-Lens Modelocking
By H.A. Haus (With 6 Figures) 3

Molecular Control Spectrometer
By Y. Yan, B.E. Kohler, R.E. Gillilan, R.M. Whitnell, K.R. Wilson, and S. Mukamel 8

Internal Motions of Proteins
By M. Karplus 13

Some Theoretical Aspects of Electron Transfer in Supermolecules
By J. Jortner and M. Bixon (With 3 Figures) 15

Femtosecond Time-Resolved Spectroscopy of Magneto-Excitons
By D.S. Chemla, J.B. Stark, and W.H. Knox (With 6 Figures) 21

High-Order Harmonic Generation in Strong Laser Fields
By A. L'Huillier and P. Balcou (With 3 Figures) 29

QED at 10^{20} W/cm^2
By A.C. Melissinos (With 6 Figures) 34

Part II Elementary Dynamics: Chemistry, Biology and Physics

Femtochemistry
By A.H. Zewail (With 6 Figures) 43

Transient Dichroism Studies of I_2 Predissociation in Solution
By N.F. Scherer, L.D. Ziegler, D. Jonas, and G.R. Fleming (With 3 Figures) 49

Investigation of the Primary Event in Vision Using 10 fs Blue-Green Optical Pulses
By R.W. Schoenlein, L.A. Peteanu, Q.W. Wang, R.A. Mathies, and C.V. Shank (With 3 Figures) 53

Mechanisms of Charge Separation in Bacterial Reaction Centers
By M.H. Vos, F. Rappaport, J.-C. Lambry, C. Rischel, J. Breton, and J.-L. Martin (With 2 Figures) 58

Coherent Phonons in Superconducting Materials
By W. Albrecht, Th. Kruse, and H. Kurz (With 3 Figures) 63

Displacive Excitation of Coherent Phonons
By T.K. Cheng, J. Vidal, H.J. Zeiger, E.P. Ippen, G. Dresselhaus, and M.S. Dresselhaus (With 1 Figure) 66

Femtosecond Time-Resolved Photodissociation of Triiodide Ions in Alcohol Solution: Directly Observed Photoinduced Vibrational Coherence of Reactants and Products
By U. Banin, A. Waldman, and S. Ruhman (With 4 Figures) 68

Vibrational Coherence in Charge Transfer
By K. Wynne, C. Galli, P.J.F. De Rege, M.J. Therien, and R.M. Hochstrasser (With 1 Figure) 71

Ultrafast Dynamics in Solution:
Wavepacket Motion and the Cage Effect in Iodine
By Y. Yan, R.M. Whitnell, K.R. Wilson, and A.H. Zewail (With 1 Figure) 74

Femtosecond Time-Resolved Ionization Spectroscopy of Polyatomic Molecules
By M. Seel and W. Domcke (With 1 Figure) 76

A Study of Nuclear Vibrational Wave Packets in Na_2 by Time- and Frequency-Resolved Fluorescence Upconversion
By I.A. Walmsley, T.J. Dunn, J. Sweetser, and C. Radzewicz (With 3 Figures) 78

Ultrafast Dynamics of Solid C_{60}
By S.L. Dexheimer, D.M. Mittleman, R.W. Schoenlein, W. Vareka, X.-D. Xiang, A. Zettl, and C.V. Shank (With 2 Figures) 81

Femtosecond Dynamics of Molecular and Cluster Ionization and Fragmentation
By T. Baumert, R. Thalweiser, V. Weiß, and G. Gerber (With 5 Figures) 83

Dephasing and Beats of Excitonic-Enhanced Transitions of J-Aggregates Measured by Femtosecond Time-Resolved Resonance CARS
By V.F. Kamalov, R. Inaba, and K. Yoshihara (With 1 Figure) 87

Excited States Dynamics of the Special Pair Dimer
By P.O.J. Scherer and S.F. Fischer (With 4 Figures) 89

Creation of an Anti-Wavepacket in a Rydberg Atom
By L.D. Noordam, H. Stapelfeldt, D.I. Duncan, and T.F. Gallagher (With 3 Figures) 92

Squeezing of the Molecular Vibrations by Femtosecond Laser Pulses
By A.V. Vinogradov and J. Janszky (With 1 Figure) 95

Part III Spectroscopy and Advances in Measurements

Spectroscopic Applications of Phase-Locked Femtosecond Pulses
By N.F. Scherer, M. Cho, L.D. Ziegler, M. Du, A. Matro, J. Cina, and G.R. Fleming (With 5 Figures) 99

Use of Piecewise Phase-Swept Pulses
to Counteract Inhomogeneous Decay in Wave Packet Interferometry
By L.W. Ungar, A. Matro, and J.A. Cina (With 1 Figure) 105

Ultrafast Nonlinear Spectroscopy with Chirped Optical Pulses
By E.T.J. Nibbering, F. de Haan, D.A. Wiersma, and K. Duppen (With 2 Figures) 107

Multiple Excitation Pulse,
Multiple Probe Pulse Femtosecond Spectroscopy
By G.P. Wiederrecht, W. Wang, K.A. Nelson, A.M. Weiner, and D.E. Leaird (With 2 Figures) 110

Stimulated Emission Pumping and Selective Excitation by Adiabatic Passage with Frequency-Modulated Picosecond Laser Pulses
By J.S. Melinger, A. Hariharan, S.R. Gandhi, and W.S. Warren (With 2 Figures) 113

A Subpicosecond Optical Sampling System
By J.D. Kafka, J.W. Pieterse, and M.L. Watts (With 2 Figures) 116

Femtosecond Sagnac Interferometry
By J.-C. Diels, P. Dorn, M. Lai, W. Rudolph, and X.M. Zhao (With 3 Figures) 120

Femtosecond Time-Gated Imaging of Translucent Objects
Hidden in Highly Scattering Media
By K.M. Yoo, B.B. Das, F. Liu, Q. Xing, and R.R. Alfano (With 2 Figures) 124

Femtosecond Waveform Processing via Spectral Holography
By A.M. Weiner, D.E. Leaird, D.H. Reitze, and E.G. Paek (With 4 Figures) 128

The Chronocyclic Representation of Ultrashort Light Pulses
By J. Paye (With 4 Figures) 133

Femtosecond Pulse Phase Measurement
by Spectrally Resolved Up-Conversion
By J.-P. Foing, J.-P. Likforman, and M. Joffre (With 3 Figures) 136

Single-Shot Measurement
of the Intensity and Phase of a Femtosecond Pulse
By D.J. Kane and R. Trebino (With 4 Figures) 138

Two-Photon Interference Measurement of Ultrafast Laser Pulses
By M. Matsuoka, Y. Miyamoto, T. Kuga, M. Baba, and Y. Li
(With 2 Figures) 140

Picosecond Single-Shot Pulse-Shape Measurement
by Stochastic Sampling of Detected Photon Times
By N. Adams, C. Bovet, E. Rossa, and A. Simonin (With 1 Figure) 142

Integrated Devices for Single Picosecond Pulse Measurements
By V. Gerbe, M. Cuzin, M.C. Gentet, and J. Lajzerowicz
(With 3 Figures) 145

The C850X Ultrafast Streak Camera: An Instrument to Study Spatially
and Temporally Subpicosecond Laser–Matter Interaction
By A. Mens, R. Sauneuf, D. Schirmann, R. Verrecchia, P. Audebert,
J.C. Gauthier, J.P. Geindre, A. Antonetti, J.P. Chambaret, G. Hamoniaux,
and A. Mysyrowicz (With 2 Figures) 147

Distortion of a 6 fs Pulse in the Focus of a BK7 Lens
By Zs. Bor and Z.L. Horváth (With 1 Figure) 150

Part IV **Tools: Sources and Amplifiers**

Modelocking, Stabilizing, and Starting Ultrashort Pulse Lasers
By E.P. Ippen (With 4 Figures) 155

17 fs Pulses from a Mode-Locked Ti:Sapphire Laser
By C.P. Huang, M.T. Asaki, S. Backus, H. Nathel, H.C. Kapteyn,
and M.M. Murnane (With 2 Figures) 160

Design Considerations for Femtosecond Ti:Sapphire Oscillators
By Ch. Spielmann, P.F. Curley, T. Brabec, E. Wintner, A.J. Schmidt,
and F. Krausz (With 3 Figures) 163

Self-Mode-Locked Cr^{3+}:$LiCaAlF_6$ and Cr^{3+}:$LiSrAlF_6$ Lasers
By A. Miller, P. Li Kam Wa, B.H.T. Chai, J.M. Evans, and W. Sibbett
(With 2 Figures) 166

Sub-50 fs Pulse Generation
from a Self-Starting CW Passively Mode-Locked Cr:$LiSrAlF_6$ Laser
By N.H. Rizvi, P.M.W. French, and J.R. Taylor (With 2 Figures) 169

CW Krypton-Laser Pumped Cr^{3+}:$LiSrAlF_6$ and Cr^{3+}:$LiSr_{0.8}Ca_{0.2}AlF_6$
Crystals Produce 150 fs Mode-Locked Pulses
By A. Miller, P. Li Kam Wa, H.S. Wang, S.L. Ayres, E.W. Van Stryland,
and B.H.T. Chai (With 3 Figures) 172

60-fs Chromium-Doped Forsterite (Cr^{4+}:Mg_2SiO_4) Laser
By A. Seas, V. Petričević, and R.R. Alfano (With 3 Figures) 174

Femtosecond Pulses from Nd:Glass Lasers
By A.J. Schmidt, M.H. Ober, M. Hofer, M.E. Fermann, F. Krausz,
T. Brabec, Ch. Spielmann, and E. Wintner (With 3 Figures) 177

A Diode-Pumped Picosecond Oscillator at 1053 nm
By I.P. Mercer, Z. Chang, M.R.G. Miller, C.N. Danson, C.B. Edwards,
and M.H.R. Hutchinson (With 3 Figures) 182

A New Intracavity Antiresonant Semiconductor Fabry-Perot
Passively Mode-Locks Nd:YLF and Nd:YAG Lasers
By U. Keller, D.A.B. Miller, G.D. Boyd, T.H. Chiu, J.F. Ferguson,
and M.T. Asom (With 3 Figures) 184

CW Mode-Locked Singly-Resonant Optical Parametric Oscillator
Pumped by a Ti:Sapphire Laser
By A. Nebel, U. Socha, and R. Beigang (With 1 Figure) 187

70 fs, High-Average Power, CW Infrared Optical Parametric Oscillator
By G. Mak, Q. Fu, and H.M. van Driel (With 2 Figures) 190

Femtosecond Intracavity Dispersion Measurements
By W.H. Knox (With 2 Figures) 192

Time Synchronization Measurements
Between Two Self-Modelocked Ti:Sapphire Lasers
By D.E. Spence, W.E. Sleat, J.M. Evans, W. Sibbett, and J.D. Kafka
(With 2 Figures) 194

Femtosecond Synchronous Pumping of Dye Lasers with <100 fs Jitter
By W.H. Knox and F.A. Beisser (With 2 Figures) 196

Development of High Average Power Femtosecond Amplifiers
Based on Ti:, Cr: and Nd:Doped Materials
By J. Squier, S. Coe, G. Mourou, D. Harter, and F. Salin 198

Femtosecond Pulse Amplification and Continuum Generation
at >250 kHz with a Ti:Sapphire Regenerative Amplifier
By T.B. Norris (With 4 Figures) 200

Millijoule Femtosecond Pulse Amplification in Ti:Al_2O_3
at Multi-kHz Repetition Rates
By F. Salin, J. Squier, G. Mourou, and G. Vaillancourt
(With 4 Figures) 203

High Repetition Rate CW Pumped Cr:LiSAF Regenerative Amplifier
By F. Balembois, P. Georges, F. Salin, G. Roger, and A. Brun
(With 4 Figures) 206

18 fs Pulse Generation
by a Single Excimer-Laser-Pumped Pulsed Dye Laser
By P. Simon, C. Jordan, and S. Szatmari (With 2 Figures) 209

Monolithic CPM Diode Lasers
By M.C. Wu, Y.K. Chen, T. Tanbun-Ek, and R.A. Logan
(With 5 Figures) 211

Ultrashort Pulse Generation from High-Power Arrays
Using Intracavity Nonlinearities
By L.Y. Pang, J.G. Fujimoto, and E.S. Kintzer (With 3 Figures) 217

100-Gbps Response of Microcavity Lasers
By H. Yokoyama, Y. Nambu, and T. Shimizu (With 2 Figures) 220

Sequential Laser Emission
in Multiple Quantum Well Vertical-Cavity Structures
By C. Tanguy, J.-L. Oudar, B. Sermage, and R. Azoulay
(With 2 Figures) 222

Experimental Analysis of Gain Modulation
in Sub-Picosecond (~0.45 ps) Mode-Locked Laser Diodes
By N. Stelmakh, J.-M. Lourtioz, and D. Pascal (With 3 Figures) 224

Generation of Stable Pulse Trains
with a Passively Modelocked Er-Fiber Laser
By M.E. Fermann, M.J. Andrejco, Y. Silberberg, and A.M. Weiner
(With 4 Figures) 227

Generation of Pairs of Solitons
in an All-Fibre, Femtosecond Soliton Source
By D.J. Richardson, V.V. Afanasjev, A.B. Grudinin, and D.N. Payne
(With 5 Figures) 229

Nonlinear Loop Mirrors in Fiber Lasers
By I.N. Duling III, C.J. Chen, P.K. Wai, and C.R. Menyuk
(With 4 Figures) 232

Temporal Characteristics of the Ytterbium–Erbium Figure-8 Laser
By I.Yu. Khrushchev, A.B. Grudinin, and E.M. Dianov
(With 3 Figures) 235

Generation of 1.7 ps Solitons by Amplification of Pulses from a Laser
Diode with Saturable Absorber in an Erbium-Doped Fibre
By I.Yu. Khrushchev, A.B. Grudinin, E.M. Dianov, D.V. Kuksenkov,
and E.L. Portnoy (With 3 Figures) 237

Part V High Intensity and Nonlinear Effects

Generation of Ultra-Intense Pulses and Applications
By G. Mourou (With 1 Figure) 241

Generation of 50 TW Femtosecond Pulses in a Nd-Glass Chain
By C. Rouyer, E. Mazataud, I. Allais, A. Pierre, and S. Seznec
(With 2 Figures) 248

All-Solid Femtosecond Oscillator–Amplifier Laser Chain
with 100 mJ per Pulse
By C. Le Blanc, G. Grillon, J.P. Chambaret, G. Boyer, M. Franco,
A. Mysyrowicz, and A. Antonetti (With 1 Figure) 251

Development of a High Intensity Femtosecond LiSAF Laser
By M.C. Richardson, P. Beaud, B.H.T. Chai, E. Miesak, Y.-F. Chen,
and V. Yanovsky (With 2 Figures) 253

Contrasted Behaviors of Stark-Induced Resonances
in Multiphoton Ionization of Krypton
By E. Mevel, R. Trainham, J. Breger, G. Petite, P. Agostini,
J.P. Chambaret, A. Migus, and A. Antonetti (With 1 Figure) 255

Phase-Dependent Ionization Using an Intense Two-Color Light Field
By D. Schumacher, M.P. de Boer, H.G. Muller, R.R. Jones,
and P.H. Bucksbaum (With 2 Figures) 257

Stabilization of Atoms in Ultra-Intense Laser Pulses: A Classical Model
By A. Maquet, T. Ménis, R. Taïeb, and V. Véniard (With 1 Figure) 259

Inertially Confined Molecular Ions
By M. Laberge, P. Dietrich, and P.B. Corkum (With 2 Figures) 261

A Femtosecond Lightning Rod
By X.M. Zhao, C.Y. Yeh, J.-C. Diels, and C.Y. Wang
(With 2 Figures) 264

Plasma Physics with Ultra-Short and Ultra-Intense Laser Pulses
By T.W. Johnston, Y. Beaudoin, M. Chaker, C.Y. Côté, J.C. Kieffer,
J.P. Matte, H. Pépin, C.Y. Chien, S. Coe, G. Mourou, and D. Umstadter
(With 1 Figure) 267

X-Rays Generated by Femtosecond Laser-Produced Plasmas
By J.P. Geindre, P. P. Audebert, A. Rousse, F. Falliès, J.C. Gauthier,
A. Mysyrowicz, G. Grillon, J.P. Chambaret, A. Antonetti, A. Mens,
R. Verrecchia, R. Sauneuf, and P. Schirman (With 2 Figures) 272

K-Shell Emission from 100 fs Laser-Produced Plasmas
Created from Porous Aluminum Targets
By R. Shepherd, D. Price, B. White, S. Gordan, A. Osterheld, R. Walling,
D. Slaughter, and R. Stewart (With 2 Figures) 275

Kilovolt X-Ray Emission from Femtosecond Laser-Produced Plasmas
By G. Jenke, H. Schüler, T. Engers, D. von der Linde, I. Uschmann,
E. Förster, and K. Gäbel (With 1 Figure) 278

Ultrafast Spectroscopy of Plasmas
Generated by Superintense Femtosecond Laser Pulses
By D. von der Linde, H. Schüler, H. Schulz, and T. Engers
(With 3 Figures) 280

Picosecond Soft-X-Ray Pulse Length Measurement
by Pump–Probe Absorption Spectroscopy
By M.H. Sher, U. Mohideen, H.W.K. Tom, O.R. Wood II,
G.D. Aumiller, D.L. Windt, W.K. Waskiewicz, J. Sugar, T.J. McIlrath,
and R.R. Freeman (With 4 Figures) 283

Photon Acceleration via Laser-Produced Ionization Fronts
By R.L. Savage Jr., R.P. Brogle, W.B. Mori, and C. Joshi
(With 5 Figures) 286

Propagation of Intense Laser Pulses in Plasmas
By E. Esarey, P. Sprangle, J. Krall, and G. Joyce (With 1 Figure) 290

Ponderomotive Steepening in Short-Scale-Length Laser-Plasmas
By D. Umstadter and X. Liu (With 2 Figures) 293

Possibility of Experimental Studies of Nonlinear Quantum
Electrodynamics Effects Using High Power Ultrashort Laser Pulses
By P.G. Kryukov (With 1 Figure) 296

Soliton-Like Self-Trapping of Three-Dimensional Patterns
By A. Barthelemy, C. Froehly, M. Shalaby, P. Donnat, J. Paye,
and A. Migus (With 9 Figures) 299

Physical Origins of the Spectral Continuum:
Self-Focusing, Self-Trapping and Cerenkov Radiation
By F. Salin, J. Watson, J.-F. Cormier, P. Georges, and A. Brun
(With 2 Figures) 306

Diffraction and Focussing of Spectral Energy in a Two-Photon Process
By B. Broers, L.D. Noordam, and H.B. van Linden van den Heuvell
(With 3 Figures) 309

Efficient Raman Conversion of Femtosecond UV Light Pulses
By K.A. Stankov and Y.-W. Lee (With 1 Figure) 311

Organic Crystalline Fiber
for Efficient Compression of Femtosecond Laser Pulses
By M. Yamashita (With 1 Figure) 313

Nonlinear Temporal Diffraction in Optical Fibers
By G.R. Boyer, M.K. Jackson, J. Paye, M.A. Franco, and A. Mysyrowicz
(With 3 Figures) 315

Generation of a Soliton Pulse Train in an Optical Fibre
Using Two CW Single-Frequency Diode Lasers
By S.V. Chernikov, J.R. Taylor, P.V. Mamyshev, and E.M. Dianov
(With 2 Figures) 318

Experimental Investigation of Dark Solitons Interaction
By Ph. Emplit, J.-P. Hamaide, and M. Haelterman (With 3 Figures) 320

Femtosecond Pulse Propagation in Erbium-Doped Single-Mode Fibers
By J.M. Hickmann, A.S.L. Gomes, C.B. de Araújo,
and A.S. Gouveia-Neto (With 3 Figures) 323

Compression of Pulses from Soliton Fibre Lasers
in a Dispersion-Decreasing Fibre
By S.V. Chernikov, D.J. Richardson, E.M. Dianov, and D.N. Payne
(With 4 Figures) 325

Part VI Metals, Surfaces and Materials

Observation of the Thermalization of Electrons in a Metal
Excited by Femtosecond Optical Pulses
By W.S. Fann, R. Storz, H.W.K. Tom, and J. Bokor
(With 2 Figures) 331

Femtosecond Thermionic Emission:
Experiment, Analytical Theory, and Particle Simulations
By M.C. Downer, D.M. Riffe, X.Y. Wang, J.L. Erskine, D.L. Fisher,
T. Tajima, and R.M. More (With 2 Figures) 335

Electron–Electron Dynamics Observed in Femtosecond Thermoreflection
Measurements on Noble Metals
By R.H.M. Groeneveld, R. Sprik, and Ad. Lagendijk (With 2 Figures) .. 338

Inversion of Single- and Two-Photon Photoelectric Sensitivities of Metals
in the Femtosecond Range
By J.P. Girardeau-Montaut, C. Girardeau-Montaut, S.D. Moustaïzis,
and C. Fotakis (With 1 Figure) 340

Femtosecond Relaxation of Plasma Excitations in Silver Films
By R.A. Höpfel, D. Steinmüller-Nethl, F.R. Aussenegg, and A. Leitner
(With 3 Figures) 342

Femtosecond Free Induction Decay
of Metal Surface Adsorbate Vibrations
By J.C. Owrutsky, J.P. Culver, M. Li, Y.R. Kim, M.J. Sarisky,
M.S. Yeganeh, R.M. Hochstrasser, and A.G. Yodh (With 1 Figure) 345

Observation of Laser-Induced Desorption of CO from Cu(111)
with 100 fs Time-Resolution
By J.A. Prybyla, H.W.K. Tom, and G.D. Aumiller (With 2 Figures) 347

Femtosecond Desorption of Molecular Oxygen from Pt(111)
By F.-J. Kao, D.G. Busch, D. Gomes da Costa, D. Cohen, and W. Ho
(With 1 Figure) 350

Femtosecond Carrier Dynamics in Solid C_{60} Films
By S.D. Brorson, M.K. Kelly, U. Wenschuh, R. Buhleier, and J. Kuhl
(With 4 Figures) 354

The Role of Covalency in Femtosecond Time-Resolved Reflectivity
of Hydrodynamically Expanding Solid Surfaces
By X.Y. Wang, H.Y. Ahn, and M.C. Downer (With 1 Figure) 357

Ultrafast Formation Processes of Self-Trapped Excitons
in Alkali Iodide Crystals under Band-to-Band Excitation
By T. Tokizaki, S. Iwai, T. Shibata, A. Nakamura, K. Tanimura,
and N. Itoh (With 2 Figures) 360

Femtosecond Self-Trapping of Interacting Electron–Hole Pairs in α-SiO_2
By W. Joosen, S. Guizard, P. Martin, G. Petite, P. Agostini,
A. Dos Santos, G. Grillon, J.P. Chambaret, D. Hulin, A. Migus,
and A. Antonetti (With 4 Figures) 362

Ultrafast Soft Mode Dynamics in Ferroelectric Crystals
By G.P. Wiederrecht, T.P. Dougherty, and K.A. Nelson
(With 3 Figures) 365

Temporal Domain Study of the Phase Transition in $PbTiO_3$:
A_1 Symmetry Investigation
By D.P. Kien, J.C. Loulergue, and J. Etchepare (With 2 Figures) 368

Femtosecond Transient Absorption Measurements
on Low Band Gap Thiophene Polymers
By A. Cybo-Ottoné, M. Nisoli, V. Magni, S. De Silvestri, O. Svelto,
G. Zerbi, and R. Tubino (With 2 Figures) 370

Effects of Crosslinking in Host Polymer
on Picosecond Optical Dephasing of Doped Dye Molecules
By S. Nakanishi, S. Fujiwara, M. Kawase, and H. Itoh
(With 3 Figures) 372

Ultrafast Relaxation of Exciton and Soliton–Antisoliton Pair
in *One-Dimensional Conjugated Polymers*
By T. Kobayashi, M. Yoshizawa, S. Takeuchi, and A. Yasuda
(With 2 Figures) 376

Polarization-Dependent Femtosecond Dynamics
of MBE-Grown Phthalocyanine Organic Thin Films
By Sandalphon, V.S. Williams, K. Meissner, N.R. Armstrong,
and N. Peyghambarian (With 3 Figures) 379

Detection of a New Strongly-Coupled Vibration Mode
During the Exciton Bleaching of Polydiacetylene
By J.M. Nunzi, C. Hirlimann, and J.F. Morhange (With 1 Figure) 381

Pressure-Induced Vibrational Relaxation and Electronic Dephasing in Molecular Crystals
By E.L. Chronister and R.A. Crowell (With 3 Figures) 384

Ultrafast Reversible Phase Changes for Optical Recording
By J. Solís, C.N. Afonso, F. Catalina, and C. Kalpouzos
(With 1 Figure) 387

Picosecond Transient Absorption and Fluorescence Emission Studies of C_{60} and C_{70} in Solution
By D. Kim, Y.D. Suh, S.K. Kim, and M. Lee (With 2 Figures) 389

Part VII Semiconductors, Confinement and Opto-Electronics

Transient Absorption-Edge Singularities in GaAs
By D. Hulin, J.-P. Foing, M. Joffre, M.K. Jackson, J.-L. Oudar,
C. Tanguy, and M. Combescot (With 3 Figures) 395

Nonthermal Distribution of Electrons in GaAs
By D. Snoke and W.W. Rühle (With 1 Figure) 399

Femtosecond Carrier–Carrier Interaction in GaAs
By T. Gong, K.B. Ucer, L.X. Zheng, G.W. Wicks, J.F. Young, P.J. Kelly,
and P.M. Fauchet (With 4 Figures) 402

Quantum Beats versus Polarization Interference: An Experimental Distinction
By M. Koch, J. Feldmann, G. von Plessen, E.O. Göbel, P. Thomas,
and K. Köhler (With 1 Figure) 405

Plasmon–Phonon Coupling and Hot Carrier Relaxation in GaAs and Low-Temperature-Grown GaAs
By R.I. Devlen, J. Kuhl, and K. Ploog (With 2 Figures) 408

Femtosecond Carrier–Carrier Interaction Dynamics in Doped GaAs
By T. Furuta and A. Yoshii (With 1 Figure) 410

Femtosecond Carrier Kinetics in Low-Temperature-Grown GaAs
By X.Q. Zhou, H.M. van Driel, A.P. Heberle, W.W. Rühle, and K. Ploog
(With 2 Figures) 412

Transient Anisotropic Luminescence and Long-Living Polarization of an Optically Excited Dense Electron–Hole Plasma
By A.L. Ivanov and H. Haug (With 2 Figures) 414

Hot Hole Capture by Shallow Acceptors in p-Type GaAs Studied by Picosecond Infrared Spectroscopy
By A. Lohner, M. Woerner, T. Elsaesser, and W. Kaiser
(With 2 Figures) 416

Ultrafast Dephasing and Interference of Coherent Phonons in GaAs
By W. Kütt, T. Pfeifer, T. Dekorsy, and H. Kurz (With 2 Figures) 418

Femtosecond, Electronically-Induced Disordering of GaAs
By J.-K. Wang, Y. Siegal, P.N. Saeta, N. Bloembergen, and E. Mazur
(With 2 Figures) 420

Laser-Induced Ultrafast Order–Disorder Transitions in Semiconductors
By K. Sokolowski-Tinten, J. Bialkowski, and D. von der Linde
(With 1 Figure) 422

Femtosecond Carrier Dynamics in InGaAsP Optical Amplifiers
By J. Mark and J. Mørk (With 1 Figure) 424

Ultrafast Nonlinear Refraction in Semiconductor Laser Amplifiers
By M. Sheik-Bahae and E.W. Van Stryland (With 3 Figures) 426

Femtosecond Luminescence Spectroscopy of Indium Phosphide
By E. Fazio and G.M. Gale (With 2 Figures) 429

Dynamics of Excitons Probed by Accumulated Photon Echo
By T. Bouma, P. Vledder, and J.I. Dijkhuis (With 1 Figure) 431

Time-Resolved Measurement of Hot Carrier Cooling Rates
in a-Si:H and a-Ge:H
By M. Wraback and J. Tauc (With 2 Figures) 433

Dephasing of the Short Exciton–Polariton Pulses
in Polar Semiconductors: The Cuprous Chloride Case
By F. Vallée, F. Bogani, and C. Flytzanis (With 3 Figures) 435

Femtosecond Electronic Dynamics of CdSe Nanocrystals
By C.V. Shank, R.W. Schoenlein, D.M. Mittleman, J.J. Shiang,
and A.P. Alivisatos (With 4 Figures) 438

Quantum Beats Spectroscopy of Exciton Spin Dynamics
in GaAs Heterostructures
By S. Bar-Ad and I. Bar-Joseph (With 3 Figures) 443

Evidence of Slow Hole Spin Relaxation
in n-Modulation Doped GaAs/AlGaAs Quantum Well Structures
By Ph. Roussignol, P. Rolland, R. Ferreira, C. Delalande, G. Bastard,
A. Vinattieri, J. Martinez-Pastor, L. Carraresi, M. Colocci, J.F. Palmier,
and B. Etienne (With 1 Figure) 446

Femtosecond Time-Resolved Four-Wave Mixing in GaAs Quantum Wells
By D.S. Kim, J. Shah, T.C. Damen, J.E. Cunningham, W. Schäfer,
and S. Schmitt-Rink (With 4 Figures) 448

Exciton Radiative Lifetimes in GaAs Quantum Wells
By R. Eccleston, J. Kuhl, W.W. Rühle, and K. Ploog
(With 2 Figures) 451

Optical Investigation of Bloch Oscillations in a Semiconductor Superlattice
By J. Feldmann, K. Leo, J. Shah, D.A.B. Miller, J.E. Cunningham, T. Meier, G. von Plessen, P. Thomas, and S. Schmitt-Rink (With 5 Figures) 454

Coherent Pulse Breakup in Femtosecond Pulse Propagation in Semiconductors
By P.A. Harten, A. Knorr, S.G. Lee, R. Jin, F. Brown de Colstoun, E.M. Wright, G. Khitrova, H.M. Gibbs, S.W. Koch, and N. Peyghambarian (With 1 Figure) 458

Absorption Saturation of the Urbach's Tail in Multiple Quantum Wells
By R. Raj, B.G. Sfez, D. Pellat, and J.L. Oudar (With 2 Figures) 460

Photon Echo Polarisation Rules in GaAs Quantum Wells
By R. Eccleston, D. Bennhardt, J. Kuhl, P. Thomas, and K. Ploog (With 3 Figures) 463

Observation of Many-Body Effects in the Femtosecond Temporal Profile of Quasi-2D Exciton Free-Induction Decay
By S. Weiss, M.-A. Mycek, J.-Y. Bigot, S. Schmitt-Rink, and D.S. Chemla (With 3 Figures) 466

Radiative Recombination of Free Excitons in GaAs Quantum Wells
By B. Sermage, K. Satzke, C. Dumas, N. Roy, B. Deveaud, F. Clerot, and D.S. Katzer (With 4 Figures) 472

Field-Enhanced GaAs/AlGaAs Waveguide Saturable Absorbers
By J.R. Karin, D.J. Derickson, R.J. Helkey, J.E. Bowers, and R.L. Thornton (With 2 Figures) 475

Picosecond Excitonic Nonlinearities in the Presence of Disorder
By S.T. Cundiff and D.G. Steel (With 3 Figures) 478

Fast Optical Nonlinearities in Semiconductor Quantum Dots
By G. Tamulaitis, R. Baltramiejūnas, S. Pakalnis, and A.I. Ekimov (With 2 Figures) 482

Terahertz Radiation from Coherent Electron Oscillations in a Double-Quantum-Well Structure
By H.G. Roskos, M.C. Nuss, J. Shah, K. Leo, D.A.B. Miller, S. Schmitt-Rink, and K. Köhler (With 3 Figures) 484

Optical Generation of Terahertz Pulses from Polarized Excitons in Quantum Wells
By P.C.M. Planken and M.C. Nuss (With 3 Figures) 487

Generation of High-Power Single-Cycle Picosecond Radiation
By D.R. Dykaar, R.R. Jones, D. You, D. Schumacher, and P.H. Bucksbaum (With 3 Figures) 490

Transient Electron Transport in GaAs Quantum Wells:
From the Ballistic to the Quasi-Equilibrium Regime
By W. Sha, J. Rhee, and T.B. Norris (With 4 Figures) 493

A Novel Free-Standing Absolute-Voltage Probe
with 2.3-Picosecond Resolution and 1-Microvolt Sensitivity
By J. Kim, S. Williamson, J. Nees, and S. Wakana
(With 3 Figures) 496

Picosecond Pseudomorphic AlGaAs/InGaAs MODFET Large-Signal
Switching Measured by Electro-Optic Sampling
By M.K. Jackson, M.Y. Frankel, J.F. Whitaker, G.A. Mourou, D. Hulin,
A. Antonetti, M. Van Hove, W. De Raedt, P. Crozat, and H. Hafdallah
(With 3 Figures) 500

Ultrafast Decay of Photodiffractive Gratings in Hetero n-i-p-i's
by Enhanced In-Plane Transport
By A.L. Smirl, D.S. McCallum, A.N. Cartwright, X.R. Huang,
T.F. Boggess, and T.C. Hasenberg (With 2 Figures) 503

Picosecond High-Sensitivity $In_xGa_{1-x}As$ Photodetectors
By S. Gupta, J.F. Whitaker, S.L. Williamson, P. Ho, J.S. Mazurowski,
and J.M. Ballingall (With 2 Figures) 505

An Ultrafast Polarization-Independent All-Optical Demultiplexer
Utilizing Induced-Frequency Shift
By T. Morioka, K. Mori, and M. Saruwatari (With 2 Figures) 508

Electrical Soliton Devices as >100 GHz Signal Sources
By E. Carman, M. Case, M. Kamegawa, R. Yu, K. Giboney,
and M. Rodwell (With 2 Figures) 511

Determination of Photonic Band Gaps and Dispersion
in Two-Dimensional Dielectric Arrays
with Ultrafast Electromagnetic Transients
By W.M. Robertson, G. Arjavalingam, R.D. Meade, K.D. Brommer,
A.M. Rappe, and J.D. Joannopoulos (With 2 Figures) 513

Part VIII **Biology: Primary Dynamics, Electron and Energy Transfer**

Ultrafast Infrared Spectroscopy of Protein Dynamics
By R.M. Hochstrasser, R. Diller, S. Maiti, T. Lian, B. Locke, C. Moser,
P.L. Dutton, B.R. Cowen, and G.C. Walker (With 5 Figures) 517

Ultrafast Near-IR Spectroscopy of Carbonmonoxymyoglobin:
The Dynamics of Protein Relaxation
By M. Lim, T.A. Jackson, and P.A. Anfinrud (With 4 Figures) 522

Energetics and Dynamics of Global Protein Motion
By R.J.D. Miller, J. Deak, S. Palese, M. Pereira, L. Richard,
and L. Schilling (With 2 Figures) 525

Investigation of the Reaction Coordinate for Ligand Rebinding
in Photoexcited Hemeproteins Using Transient Raman Spectroscopy
By H. Zhu, R. Lingle, Jr., X. Xu, and J.B. Hopkins
(With 2 Figures) 528

Resonance Raman Studies of Electronic and Vibrational Relaxation
Dynamics in Heme Proteins
By P.M. Champion, J.T. Sage, and P. Li 533

Molecular Processes in the Primary Reaction
of Photosynthetic Reaction Centers
By W. Zinth, C. Lauterwasser, U. Finkele, P. Hamm, S. Schmidt,
and W. Kaiser (With 3 Figures) 535

Femtosecond Spontaneous Emission Studies
of Photosynthetic Bacterial Reaction Centers
By S.J. Rosenthal, M. Du, X. Xie, T.J. DiMagno, M.E. Schmidt,
J.R. Norris, and G.R. Fleming (With 1 Figure) 539

Subpicosecond Emission Studies of Bacterial Reaction Centers
By P. Hamm and W. Zinth (With 1 Figure) 541

Picosecond Fluorescence Kinetics of Purple Bacterial Reaction Centers
By M.G. Müller, K. Griebenow, and A.R. Holzwarth (With 2 Figures) . . 543

Primary Radical Pair Formation in Photosystem-Two Reaction Centres
By D.R. Klug, J.R. Durrant, G. Hastings, Q. Hong, D.M. Joseph,
J. Barber, and G. Porter (With 3 Figures) 546

Energy Transfer and Primary Charge Separation in Heliobacteria
by Picosecond Transient Absorption Spectroscopy
By P.I. van Noort, T.J. Aartsma, and J. Amesz
(With 3 Figures) 549

Excitation Energy Transfer in Mutants of *Rb. sphaeroides*:
The Effects of Changes in the Core Antenna Size
By L.M.P. Beekman, R.W. Visschers, K.J. Visscher, B. Althuis, W. Barz,
D. Oesterhelt, V. Sundström, and R. van Grondelle
(With 3 Figures) 552

Femtosecond Excitation Transfer in Allophycocyanin
By A.V. Sharkov, E.V. Khoroshilov, I.V. Kryukov, P.G. Kryukov,
T. Gillbro, R. Fischer, and H. Scheer (With 1 Figure) 555

Femtosecond Förster Energy Transfer over 20 Å
in Phycoerythrocyanin (PEC) Trimers
By L.O. Palsson, T. Gillbro, A. Sharkov, R. Fischer, and H. Scheer
(With 1 Figure) 557

Ultrafast Energy Transfer Within the Light-Harvesting Antenna of Photosynthetic Purple Bacteria
By K.J. Visscher, V. Gulbinas, R.J. Cogdell, R. van Grondelle, and V. Sundström (With 2 Figures) 559

Femtosecond Dynamics in Rhodopsin
By T. Kobayashi, M. Taiji, K. Bryl, M. Nakagawa, and M. Tsuda (With 2 Figures) 562

Subpicosecond Time-Resolved Spectroscopy of Halorhodopsin and Comparison with Bacteriorhodopsin
By H. Kandori, K. Yoshihara, H. Tomioka, H. Sasabe, and Y. Shichida (With 3 Figures) 566

Part IX Chemistry: Electron and Energy Transfer, and Solvation Dynamics

---

Femtosecond Intermolecular Electron Transfer: Dye in Weakly Polar Electron-Donating Solvent
By K. Yoshihara, A. Yartsev, Y. Nagasawa, H. Kandori, A. Douhal, and K. Kemnitz (With 3 Figures) 571

Ultrafast Studies and Simulations on Direct Photoinduced Electron Transfer in the Betaines
By A.E. Johnson, N.E. Levinger, G.C. Walker, and P.F. Barbara (With 3 Figures) 576

Picosecond Infrared Study of Ultrafast Electron Transfer and Vibrational Energy Relaxation in $[(NC)_5RU^{II}CNRu^{III}(NH_3)_5]^{1-}$
By P.O. Stoutland, S.K. Doorn, R.B. Dyer, and W.H. Woodruff (With 1 Figure) 579

Ultrafast Studies on Intervalence Charge Transfer
By K. Tominaga, D.A.V. Kliner, J.T. Hupp, and P.F. Barbara (With 1 Figure) 582

Picosecond Infrared Study of Intramolecular Energy Transfer in $[(phen)(CO)_3Re^{I}(NC)Ru^{II}(CN)(bpy)_2]^+$
By R.B. Dyer, K.A. Peterson, K.C. Gordon, W.H. Woodruff, J.R. Schoonover, T.J. Meyer, and C.A. Bignozzi (With 1 Figure) 585

Noise-Induced Intramolecular Electron Transfer Processes in Polar Media
By P.O.J. Scherer 587

Femtosecond Proton Transfer in the Electronic Ground State of Vibrationally Hot Molecules
By T. Elsaesser, W. Frey, and M.T. Portella (With 2 Figures) 589

Solvent Effects on the Fast Proton Transfer of 3-Hydroxyflavone
By B.J. Schwarz, L.A. Peteanu, and C.B. Harris (With 3 Figures) 592

Time-Resolved Charge Separation
in Acceptor-Substituted Anthrylpolyenes
By H. Port, G. Quapil, H.C. Wolf, F. Effenberger, C.-P. Niesert,
R. Buhleier, Z. Gogolak, and J. Kuhl (With 2 Figures) 596

Vibrationally Unrelaxed cis-Stilbene Photoproducts Examined Through
Two-Color UV Pump-Probe Anti-Stokes Raman Spectroscopy
By D.L. Phillips, J.-M. Rodier, and A.B. Myers (With 4 Figures) 598

Vibrational Energy Redistribution and Relaxation
in the Photoisomerization of cis-Stilbene
By R.J. Sension, S.T. Repinec, A.Z. Szarka, and R.M. Hochstrasser
(With 2 Figures) 601

Photoisomerization of cis-Stilbene in Compressed Solvents
By L. Nikowa, D. Schwarzer, J. Troe, and J. Schroeder
(With 2 Figures) 603

Ultrafast Torsional Dynamics in Adsorbates: An SSHG Study
By M.J.E. Morgenthaler and S.R. Meech (With 1 Figure) 606

Barrierless Photochemical Isomerization
By U. Åberg, E. Åkesson, I. Fedchenia, and V. Sundström
(With 2 Figures) 608

Femtosecond Molecular Dynamics in Liquids
By D.A. Wiersma, E.T.J. Nibbering, and K. Duppen
(With 4 Figures) 611

Femtosecond Solvent Dynamics
Studied by Time-Resolved Fluorescence and Transient Birefringence
By S.J. Rosenthal, N.F. Scherer, M. Cho, X. Xie, M.E. Schmidt,
and G.R. Fleming (With 2 Figures) 616

Adiabatic and Nonadiabatic Effects in Solvation Dynamics
By E. Neria and A. Nitzan (With 1 Figure) *618*

Excited-State Processes of 7-Azaindole
By M. Négrerie, F. Gai, J.-C. Lambry, J.-L. Martin, and J.W. Petrich
(With 1 Figure) 621

Excited-State Proton Transfer and Hydrogen-Bonding Dynamics in
7-Azaindole: Time-Resolved Fluorescence and Computer Simulation
By C.F. Chapman, T.J. Marrone, R.S. Moog, and M. Maroncelli 624

Transient Hole Burning Studies of Electronic State Solvation:
Phonon and Structural Contributions
By J. Yu, J.T. Fourkas, and M. Berg (With 2 Figures) 626

Subpicosecond Study of the Dynamic Processes in Push-Pull Styrenes and the Role of Solvation
By P. Hébert, G. Baldacchino, T. Gustavsson, V. Kabelka, P. Baldeck, and J.-C. Mialocq (With 3 Figures) 628

Picosecond Studies of Charge Transfer States in "Push-Pull" Linear Diphenyl Polyenes: Experimental Evidence for TICT and Bicimer States
By J.M. Viallet, F. Dupuy, R. Lapouyade, W.Q. Zheng, and C. Rullière (With 2 Figures) 631

Features of the Dual Fluorescence of 4-N,N-dialkylaminoalkylbenzoates in Alkanes
By M.C.C. de Lange, D.T. Leeson, A.H. Huizer, and C.A.G.O. Varma (With 1 Figure) 634

Investigation of Fast Relaxation Processes in Non-Fluorescent Rhodamine Dyes
By P. Plaza, N.D. Hung, M.M. Martin, Y.H. Meyer, and W. Rettig (With 1 Figure) 636

Femtosecond Photodissociation of Aromatic Disulfides Followed by Solvent Relaxation
By N.P. Ernsting (With 4 Figures) 638

Femtosecond Dynamics of C–O Bond Cleavage of a Spirooxazine Photochromic Reaction
By N. Tamai and H. Masuhara (With 2 Figures) 641

Dynamics of Molecular Rotation at the Air/Water Interface by Time-Resolved Second-Harmonic Generation
By A. Castro, D. Zhang, and K.B. Eisenthal (With 5 Figures) 644

Energy Relaxation and Redistribution in Large Molecules in Solution on Ultrafast Time Scales
By C.B. Harris, J.C. King, K.E. Schultz, B.J. Schwartz, and J.Z. Zhang (With 2 Figures) 650

Photodissociation and Recombination Dynamics of I_2^- in Solution
By J.C. Alfano, D.A.V. Kliner, A.E. Johnson, N.E. Levinger, and P.F. Barbara (With 3 Figures) 653

Probing the Microscopic Molecular Environment in Liquids with Femtosecond Fourier-Transform Raman Spectroscopy
By D. McMorrow, S.K. Kim, J.S. Melinger, and W.T. Lotshaw (With 3 Figures) 656

The Homogeneity of Liquid Phase Vibrational Line Broadening from Raman Echo Experiments
By L.J. Muller, D. Vanden Bout, and M. Berg (With 2 Figures) 658

Excited State Photoreactions of Chlorine Dioxide in Solution
By R.C. Dunn and J.D. Simon (With 2 Figures) 661

Bimolecular Reactions are Power-Full
By A. Masad, S.Y. Goldberg, D. Huppert, and N. Agmon
(With 4 Figures) 664

Dynamics and Mechanism of Cu-Porphyrin Triplet Quenching
Through Liganding by Oxygen-Containing Solvents
By V.S. Chirvony and R. Gadonas 667

Fast Processes in Liquid Alkane Photolysis
Above the Ionization Threshold
By M. Sander, U. Brummund, K. Luther, and J. Troe (With 1 Figure) .. 669

Index of Contributors 671

Molecular Processes in the Primary Reaction of Photosynthetic Reaction Centers

W. Zinth[1], *C. Lauterwasser*[1], *U. Finkele*[2], *P. Hamm*[1], *S. Schmidt*[2], *and W. Kaiser*[2]

[1]Institut für Medizinische Optik der Universität München,
Barbarastr. 16/IV, W-8000 München 40, Fed. Rep. of Germany
[2]Physik Department E 11 der Technischen Universität München,
W-8046 Garching, Fed. Rep. of Germany

Abstract: The primary electron transfer is investigated for wildtype reaction centers from Rhodobacter sphaeroides, mutant reaction centers and reaction centers with modified bacteriochlorophyll . Experimental results are presented which strongly support the idea that the electron transfer is stepwise involving the accessory bacteriochlorophyll as a real intermediate electron carrier.

1. Introduction

The energy converting processes of bacterial photosynthesis start in a large chromoprotein called reaction center (RC). At first light energy leads to electronic excitation of a chromophore. Subsequently the electronic excitation initiates an electron transfer (ET) via several acceptor molecules. Finally the electron reaches the quinone Q_B. Further secondary transfer processes involve diffusive motion of protons and large organic molecules. Schematically the structural arrangement of the electron carrying pigments in the RC's is shown in Fig. 1 /1, 2/. The pigments are incorporated in two branches (A and B) related by an approximate C_2 symmetry. The two branches cross at two strongly interacting bacteriochlorophyll molecules forming the special pair P which acts as a primary electron donor. Subsequently each branch contains a monomeric bacteriochlorophyll molecule B_A and B_B, a bacteriopheophytin (H_A, H_B) and a quinone (Q_A, Q_B). Various experiments have revealed that the two pigment branches are not equivalent and that the reactive electron transfer uses the A branch.

The very first reaction processes include the initial charge separation and the ET until the bacteriopheophytin H_A. These events take several picoseconds /3-9/. In the next step the electron reaches within approximately 200 ps the quinone Q_A. The secondary quinone Q_B is reduced only much slower on the 10^{-6} s time scale. Transient absorption spectroscopy of the

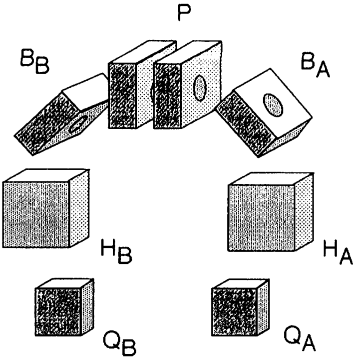

Fig. 1: Schematic of the molecular arrangement of the four bacteriochlorophylls (P, B_A, B_B), the two bacteriopheophytins (H_A, H_B) and the two quinones (Q_A, Q_B) in reaction centers

Springer Series in Chemical Physics, Vol. 55 Ultrafast Phenomena VIII
Editors: J.-L. Martin · A. Migus · G.A. Mourou · A.H. Zewail
© Springer-Verlag Berlin Heidelberg 1993

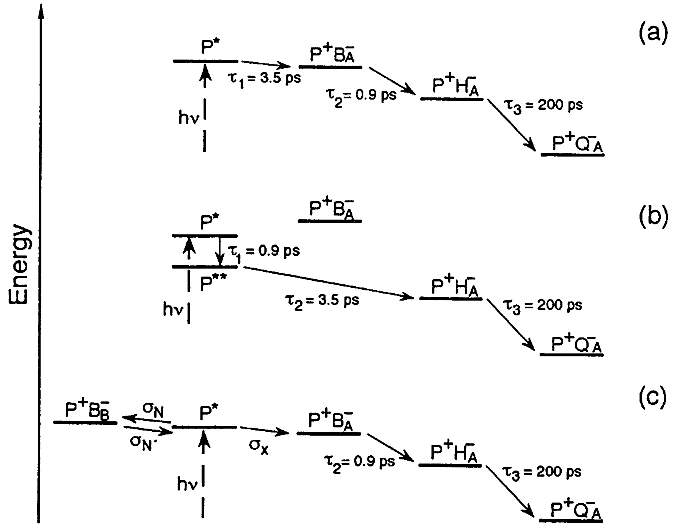

Fig. 2: Reaction models for the primary electron transfer

primary reaction dynamics at room temperature exhibit one time constant around 3.5 ps (in the literature values are reported between 2.8 ps and 4 ps /3-9/) related to the decay of the excited electronic state P* and a weak subpicosecond kinetic (0.9 ps in Rb. sphaeroides) best seen in the absorption range of the BChl and the BChl anion /7-9/. Until now no generally accepted molecular interpretation of the fast kinetic component exists /10-12/. Two reaction models are currently discussed (see Fig. 2a and b):

The structural arrangement of the reaction centers strongly suggests the stepwise electron transfer model of Fig. 2a: According to this model the electronically excited state P* of the special pair decays with the time constant of 3.5 ps. Simultaneously an electron is transferred from the special pair to the monomeric bacteriochlorophyll B_A. The second electron transfer is faster and carries the electron with a time constant of 0.9 ps to the bacteriopheophytin H_A. Finally the 200 ps process generates the radical pair $P^+Q_A^-$ where the electron has reached the first quinone.

In model 2b the fast time constant of 0.9 ps is assigned to an excited state relaxation process of the special pair. This process should be vibrational relaxation from the initially populated Franck-Condon-state. In this reaction model the first electron transfer drives the electron with a time constant of 3.5 ps directly to the bacteriopheophytin H_A. This fast long-distance electron transfer is only possible if the monomeric BChl B_A is involved as a virtual intermediate in a superexchange interaction. In this case the energy level of the corresponding radical pair $P^+B_A^-$ is higher than the energy of P*. From extensive experimental studies the absorption spectra of the different intermediates could be calculated for both models /7-9/. These data were fully consistent with the molecular interpretation of the respective model.

In this paper we will present transient absorption data on RC of Rb. sphaeroides where additional information on the reaction model is obtained by: (i) biochemical modifications of the RC and (ii) changing the temperature of the sample.

2. Results and Discussion

Measurements on low temperature RC are performed on quinone depleted RC from the carotenoid free strain R26.1. The preparation of RC where BChl a at the accessory position B_A is exchanged to approximately 70 % by [3-vinyl]-13^2-OH-BChl a is described in Ref. 13. The time resolved absorption experiments are performed using the excite and probe technique with weak subpicosecond pulses (pulse duration $\simeq$ 150 fs) generated by a laser-amplifier-system

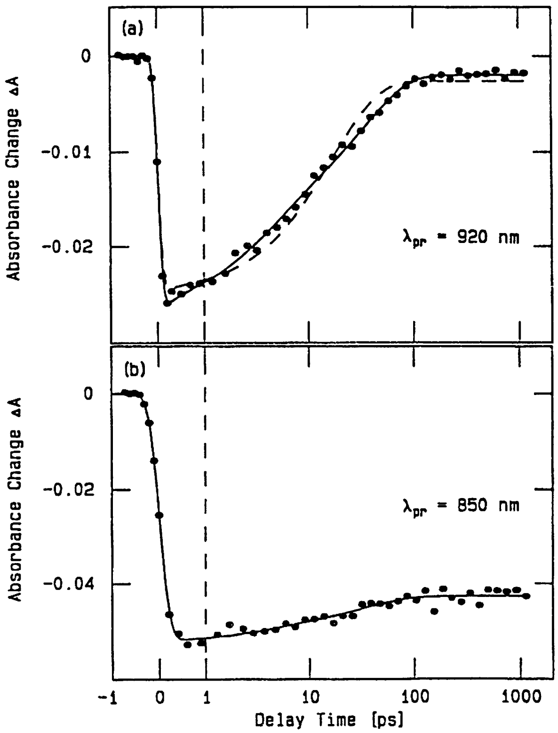

Fig 3: Transient absorption data on [3-vinyl]-13^2-OH-RC-preparations. Probing in the gain region at λ = 920 nm (a) and in special pair absorption band λ = 850 nm (b)

with a repetition rate of 10 Hz. The temporal width of the instrumental response function is below 300 fs. Details of the experimental system are described in reference /14/.

Upon lowering the temperature of the RC preparation the picosecond kinetics become faster /14, 15/. The decay of the gain having a time constant of around 3.5 ps at room temperature speeds up to 1.4 ps at 25 K. The 0.9 ps kinetic component also accelerates at lower temperatures. At 25 K a value of 0.3 ps is reached. Throughout the whole temperature range from 300 K to 25 K the spectral signature of the fast component does not change.

Experiments on [3-vinyl]-13^2-OH-BChl a containing RC's are shown in Fig. 3. The modification due to the 3 vinyl group is expected to change the redox potential of the BChl and the energy of the radical pair state P^+B^-. This change should have pronounced consequences on the ET when the accessory BChl B_A is involved. Indeed, one finds a strong slowing down of the decay of P* (see Fig. 3a for a measurement in the gain region). The experimental data indicate that the RC's containing [3-vinyl]-13^2-OH-BChl a have a decay time of P* of 32 ps. Fig. 3b, measured at a wavelength where the P absorption is strong, shows a long-lasting bleaching of P. These observations prove that the exchange leads to RC's which are still photochemically active but where the ET-step out of P* is slowed down by a factor of ten. In the [3-vinyl]-13^2-OH-BChl a containing RC's the 0.9 ps component is not visible. Experimental indications exist that a related process appears with a longer time constant in the 5 ps domain. The disappearance of the 0.9 ps component can be taken as a strong indication that the 0.9 picosecond process in wildtype RC is not related to vibrational relaxation of P* since P* is unchanged upon modifying B. This finding argues against the superexchange electron transfer of model 2b.

Additional support of the stepwise model of Fig. 2a comes from the low temperature hole-burning experiments where narrow holes related to a $\tau >$ 1ps process are observed. According to these experiments the 0.3 ps process observed in transient absorption spectroscopy can not be the first reaction. As a consequence the 0.3 ps time constant (and due to the smooth temperature dependence the 0.9 ps time at room temperature) must be related to the second reaction step.

Other important experimental information is obtained from transient absorption spectroscopy of an antenna deficient mutant (strain U43, pTXA6-10) of Rb. capsulatus. Here whole chromatophores are investigated instead of isolated RC's. The experiments exhibit the same subpicosecond component as observed in the RC preparation. This finding clearly indicates that the subpicosecond component is not an artefact due to the preparation procedure. Recently emission experiments on RC have shown that the 3.5 ps kinetic component of wildtype RC has to be split into a 2.3 ps and a 7 ps process/17/. Within the scope of the stepwise ET model this biexponentiality can be explained by a transient ET to the acccessory bacteriochlorophyll on the B branch as indicated in scheme C of Fig. 2. According to this interpretation the ET on the B branch would be blocked efficiently only between B_B and H_B.

In conclusion, we have shown that the primary processes in photosynthetic RC can be explained by a stepwise electron transfer from the special pair over the different electron carrying pigments. The distance between the pigments is small enough to allow fast and efficient electron transfer in the stepwise model.

Acknowledgement: The author thank H. Scheer and G. Drews for providing us with high quality preparations.

References

1. J.Deisenhofer, H.Michel, EMBO J. 8, 2149 (1989).
2. C.H.Chang, D.Tiede, J.Tang, U.Smith, J.Norris, M.Schiffer, FEBS Letters 205, 82 (1986).
3. N.W.Woodbury, M.Becker, D.Middendorf, W.W.Parson, Biochem. 24, 7516 (1985).
4. J.Breton, J.L.Martin, A.Migus, A.Antonetti, A.Orszag, Proc. Natl. Acad. Sci. US 83, 5121 (1986).
5. J.L.Martin, J.Breton, A.J.Hoff, A.Migus, A.Antonetti, Proc. Natl. Acad. Sci. US 83, 957 (1986).
6. C.Kirmaier, D.Holten, W.W.Parson, Biochim. et Biophys. Acta 810, 49 (1985).
7. W.Holzapfel, U.Finkele, W.Kaiser, D.Oesterhelt, H.Scheer, H.U.Stilz, W.Zinth, Chem. Phys. Letters 160, 1 (1989).
8. W.Holzapfel, U.Finkele, W.Kaiser, D.Oesterhelt, H.Scheer, H.U.Stilz, W.Zinth, Proc. Natl. Acad. Sci. US 87, 5168 (1990).
9. K.Dressler, E.Umlauf, S.Schmidt, P.Hamm, W.Zinth, S.Buchanan, H.Michel, Chem. Phys. Letters 183, 270 (1991).
10. M.Plato, K.Möbius, M.E.Michel-Beyerle, M.Bixon, J.Jortner, J. Am. Chem. Soc. 110, 7279 (1988).
11. R.A.Marcus, Chem. Phys. Letters 133, 471 (1987).
12. M.Bixon, J.Jortner, M.E.Michel-Beyerle, Biochim. et Biophys. Acta 1056, 301(1991).
13. A. Struck, E. Cmiel, I. Katheder, H. Scheer, FEBS Lett. 268, 180 (1990).
14. C.Lauterwasser, U. Finkele, H. Scheer, W. Zinth; Chem. Phys. Letters 183, 471 (1991).
15. G.R.Fleming, J.L.Martin, J.Breton, Nature 333, 190 (1988).
16. S.G. Johnson, D. Tang, R. Jankowiak, J.M. Hayes, G. J. Small, J. Phys. Chem. 93, 5953 (1989) .
17. P. Hamm, W. Zinth, (1992) same proceedings.